



HAL
open science

Finite-temperature stability of hydrocarbons: Fullerenes vs flakes

Ariel Francis Perez-Mellor, Pascal Parneix, Florent Calvo, Cyril Falvo

► **To cite this version:**

Ariel Francis Perez-Mellor, Pascal Parneix, Florent Calvo, Cyril Falvo. Finite-temperature stability of hydrocarbons: Fullerenes vs flakes. *Journal of Chemical Physics*, 2022, 157 (17), pp.171102. 10.1063/5.0122561 . hal-04288567

HAL Id: hal-04288567

<https://hal.science/hal-04288567>






Submitted on 16 Nov 2023

HAL is a multi-disciplinary open access archive for the deposit and dissemination of scientific research documents, whether they are published or not. The documents may come from teaching and research institutions in France or abroad, or from public or private research centers.

L'archive ouverte pluridisciplinaire **HAL**, est destinée au dépôt et à la diffusion de documents scientifiques de niveau recherche, publiés ou non, émanant des établissements d'enseignement et de recherche français ou étrangers, des laboratoires publics ou privés.

RAPID COMMUNICATION | NOVEMBER 01 2022

Finite-temperature stability of hydrocarbons: Fullerenes vs flakes

Ariel Francis Perez-Mellor ; Pascal Parneix ; Florent Calvo ; Cyril Falvo  



J. Chem. Phys. 157, 171102 (2022)

<https://doi.org/10.1063/5.0122561>



View
Online



Export
Citation

CrossMark

Finite-temperature stability of hydrocarbons: Fullerenes vs flakes

Cite as: *J. Chem. Phys.* **157**, 171102 (2022); doi: [10.1063/5.0122561](https://doi.org/10.1063/5.0122561)

Submitted: 24 August 2022 • Accepted: 3 October 2022 •

Published Online: 1 November 2022



View Online



Export Citation



CrossMark

Ariel Francis Perez-Mellor,^{1,a)}  Pascal Parneix,¹  Florent Calvo,²  and Cyril Falvo^{1,2,b)} 

AFFILIATIONS

¹Institut des Sciences Moléculaires d'Orsay (ISMO), CNRS, Université Paris Saclay, 91405 Orsay, France

²Univ. Grenoble Alpes, CNRS, LIPhy, 38000 Grenoble, France

^{a)}Present address: Department of Physical Chemistry, University of Geneva, 30 Quai Ernest-Ansermet, 1211 Geneva 4, Switzerland.

^{b)}Author to whom correspondence should be addressed: cyril.falvo@universite-paris-saclay.fr

ABSTRACT

The effects of a finite temperature on the equilibrium structures of hydrocarbon molecules are computationally explored as a function of size and relative chemical composition in hydrogen and carbon. Using parallel tempering Monte Carlo simulations employing a reactive force field, we find that in addition to the phases already known for pure carbon, namely, cages, flakes, rings, and branched structures, strong changes due to temperature and the addition of little amounts of hydrogen are reported. Both entropy and the addition of moderate amounts of hydrogen favor planar structures such as nanoribbons over fullerenes. Accurate phase diagrams are proposed, highlighting the possible presence of multiple phase changes at finite size and composition. Astrophysical implications are also discussed.

Published under an exclusive license by AIP Publishing. <https://doi.org/10.1063/5.0122561>

I. INTRODUCTION

Carbon systems from small clusters to bulk matter exhibit a large variety of structures and properties due to the ability of carbon to form single, double, and triple bonds. In the solid state, carbon is present as graphite and diamond but can also be amorphous or even porous, making it useful for separation or energy conversion purposes.¹ Carbon also drives a huge interest as the key to advanced low-dimensional materials, such as nanotubes or graphene. Despite being the focus of extensive research for many decades,^{2–6} many properties of carbon systems remain poorly understood. This is particularly true for carbon systems under extreme conditions, such as clusters in the gas phase⁴ or liquid carbon.⁷

In the dilute limit, carbon clusters and hydrocarbon molecules play an important role in astrochemistry. For example, the presence of polycyclic aromatic hydrocarbons (PAHs) in the interstellar medium (ISM) was suggested nearly forty years ago through the observation of the so-called aromatic infrared bands (AIBs).^{8–10} In addition, a variety of pure carbon clusters have now been conclusively observed in the ISM, ranging from small carbon chains^{11,12} up to C₆₀ and C₇₀ fullerenes.^{13,14} However, a much larger variety of hydrocarbon systems is expected to be present under astrophysical conditions and contribute to different spectral features of the ISM,

such as the diffuse interstellar bands (DIBs), the ultraviolet (UV) bump, and the AIBs themselves.^{15–23}

The allotropy of carbon conveys to the nanoscale, as pure carbon clusters display a large variety of structures and can be found as chains, rings, flakes (mostly planar, aromatic structures), and cages (which include fullerenes).^{2–4,24} Quite a number of theoretical studies using different potential energy surfaces have focused on low-energy structures, typically explored as a function of the number of carbon and hydrogen atoms.^{25–38} While these studies generally highlighted the dependence of the results on the specific energy model, they all concluded that for small pure carbon clusters ($N_C \lesssim 8$), the lowest isomers are linear chains, followed by rings ($8 \lesssim N_C \lesssim 16$), flakes ($16 \lesssim N_C \lesssim 24$), and fullerenes ($N \gtrsim 24$). Additional hydrogen atoms strongly alter the stability of these structures.³⁸ In particular, it is expected that fullerenes, which are the most stable structures for large clusters, become less stable as hydrogen atoms are added. Conversely, flakes structures (which include the PAH family) should become edge stabilized by hydrogenation much more conveniently than fullerenes.

Besides structural investigations, only a few studies were aimed at including the effects of a finite temperature or excess energy on isolated hydrocarbon compounds.^{39–41} In their seminal computational study, Kim and Tománek³⁹ showed using a tight-binding

model that fullerenes exhibit multiple phase transitions upon heating. After first losing their well-defined, highly symmetric structures forming the low-temperature solid state, a more floppy phase arises that still consists of cages but with increasing amounts of topological defects. Upon further increasing the temperature, the fullerenes undergo dramatic phase changes at 4000 K into a so-called pretzel phase corresponding to interconnected carbon rings and eventually into multiple connected chains, until they finally dissociate at even higher temperatures. The pretzel phase transition was suggested as the equivalent of the melting phase transition in bulk carbon.³⁹ While these temperatures are notably high for laboratory experiments, they can be reached rather easily under astrophysical conditions, even for small isolated molecules that undergo photonic excitation in the UV range: a single 10 eV photon absorbed by a 60-atom molecule is already equivalent to 700 K heating.

To a large extent, the phenomenology of fullerene melting explored by Kim and Tománek³⁹ is consistent with the structural diversity in carbon clusters recently addressed more extensively through systematic sampling methods.^{18,41,42} However, while the importance of sp^2 -dominated cages at low temperature or energy and sp^1 -dominated pretzels and chains at higher temperatures could be confirmed, the phase of flakes, still sp^2 dominated but with a much more open character, has remained relatively overlooked. However, flakes and graphene nanoribbons are important motifs of carbon at the nanoscale, not only for their use as building blocks for innovative materials^{43–45} but also, in the astrochemical context, as possible intermediates in the formation of fullerenes themselves.^{46,47} Flakes and nanoribbons can be stabilized by the presence of hydrogen, acting to protect the unsaturated and peripheral carbon atoms that are specific to this rather open phase. In view of the abundance of hydrogen in the Universe, it is also essential to determine its effects on the thermodynamics of dilute carbon matter and how the combined influences of temperature, cluster size, and relative amount of hydrogen affect the preferred structures. Our goal in this Communication is to bridge this gap with our current understanding that is mostly limited to pure carbon, by means of atomistic modeling that includes exhaustive sampling methods and a reactive potential relevant for hydrocarbon compounds. In particular, by designing appropriate order parameters, we are able to delineate the stability conditions of cages, pretzels, and chains, but also of the elusive flakes, through entire finite size phase diagrams.

II. THEORETICAL METHODS

Carbon clusters are characterized by a highly rugged energy landscape whose exploration requires efficient computational approaches. In this Communication, we use the well-established parallel tempering Monte Carlo (PTMC) method in the canonical ensemble.⁴⁸ To prevent irreversible dissociation that is likely to occur at high enough temperatures, we further impose a connectivity criterion to the structures sampled during the Monte Carlo process, rejecting disconnected configurations. Here, simple distance criteria were used to define connectivity, with $d_{CC} = 3 \text{ \AA}$ for carbon–carbon distances and $d_{CH} = d_{HH} = 2 \text{ \AA}$ for distances involving hydrogen atoms. These values were chosen significantly larger than typical chemical bond distances in such a way that bond breaking and

formation are still allowed, while also avoiding irreversible dissociation. As a result, at high temperatures, the presence of dissociated structures is expected, but with fragments that remain close to each other. This also provides a means of quantifying the stability of the fully connected structures in the simulations.

Following our earlier work,¹⁸ we use the second-generation reactive empirical bond order (REBO) potential⁴⁹ to describe atomic interactions between carbon and hydrogen atoms in the clusters. This reactive force field was originally designed to describe the energetic properties of isolated hydrocarbon molecules and various carbon materials in condensed phases. In particular, it has been used to describe the lowest-energy structures of carbon clusters³³ with good agreement with respect to other methods that explicitly account for electronic structure, such as the density-functional-based tight-binding (DFTB) method.³²

PTMC simulations were performed for 12 different pure carbon clusters with sizes in the range of 20–80 atoms. Hydrogenated clusters were also studied for specific amounts of carbon, namely, 28 or 60 carbon atoms and 0–12 or 0–20 hydrogen atoms, respectively. For all systems, the PTMC simulations employed a total of 28 or 32 replicas with temperatures allocated according to a geometric progression, additional temperatures being inserted around the main melting phase change to further enhance sampling. The complete numerical details of the PTMC simulations are provided in the [supplementary material](#). The raw data from the PTMC simulations were then processed using a version of the weighted histogram analysis method⁵⁰ based on an implementation from Poteau *et al.*⁵¹ to yield the various properties of interest as a continuous function of temperature.

To interpret the thermodynamical observables and connect their features to the underlying structural properties of the clusters, and also to merely assign the phases themselves, a number of order parameters were employed. Following previous works,^{18,52,53} the shape of the clusters is characterized using three rotationally invariant parameters derived from the successive moments of the gyration tensor, namely, the gyration radius R_g , the asphericity A_3 , and the prolateness S of the atomic distribution. Altogether, these quantities, fully explicated in the [supplementary material](#), measure the geometrical extension, the similarity to a sphere, a disk, or a chain. In addition to providing insight into the geometrical extension of the system for a given size, the gyration radius is also naturally expected to be particularly sensitive to size itself. In two-dimensional flakes, but also in hollow (single shell) cages, R_g should scale with the number of carbon atoms N_C as $\sqrt{N_C}$. A similar scaling is expected for branched structures according to polymers theory.⁵⁴ To better compare R_g across system sizes, we thus employ a scaled gyration radius $\tilde{R}_g = R_g/\sqrt{N_C}$. For hydrogen-containing systems, and since our interest lies in the effects of hydrogen on the carbon nanostructure, hydrogen atoms are ignored when calculating the gyration tensor and the same definition is used for \tilde{R}_g .

In addition to their geometrical features, clusters were also characterized in terms of their chemical bonding. Here, we have used simple coordination parameters as measures of hybridization of the carbon atoms, defining the fractions $\tilde{N}_\alpha = N_\alpha/N_C$ of such atoms having a fixed coordination number α equal two or three. We use the definition of the atomic coordination introduced in the REBO

potential itself,⁴⁹ which for any carbon atom i yields a (real) number N_i^C of nearest neighbors as

$$N_i^C = \sum_{j \neq i}^{N_C} f_{CC}^c(r_{ij}), \quad (1)$$

where $f_{CC}^c(r_{ij})$ is a smooth cutoff function acting between 1.7 and 2.0 Å (see Ref. 49).

III. RESULTS

A. Pure carbon clusters

First-order finite-size phase changes are conveniently identified by sudden variations in the system energy upon increasing temperature. With increasing size, these energy variations become sharper until an abrupt discontinuity (the latent heat) is recovered in the bulk limit of the proper first-order phase transition. As a result, the specific heat, which corresponds to the derivative of the internal energy with respect to temperature, may exhibit one or several prominent peaks at the corresponding transition temperatures in finite size systems as well. Figure 1(a) shows the specific heat as a

function of temperature for the various carbon clusters, normalized at their maxima for a better comparison across sizes.

For the larger clusters C_{60} , C_{70} , and C_{80} , only a single peak is found at $T = 3390$ K, $T = 3580$ K, and $T = 3740$ K, respectively, suggesting that these clusters experience only a single phase change. This phase change corresponds to melting, as already analyzed in Ref. 39. In C_{60} , the peak appears slightly asymmetric with a clear shoulder on the low-temperature side. In the smaller clusters containing 30–50 atoms, an additional peak is found in the specific heat, which becomes increasingly separated from the main peak as size decreases. Moreover, the two features shift to lower temperatures as size decreases. In C_{34} and below, a third feature can be perceived at temperatures higher than the main peak, in the 3000–4000 K range, which, furthermore, becomes increasingly well-defined as the clusters become smaller.

To assist in the interpretation of these thermal features, Figs. 1(b) and 1(c) show the temperature dependence of the average scaled radius of gyration \tilde{R}_g and the proportion \tilde{N}_3 of triply coordinated atoms. The three phase changes identified in the specific heat are clearly seen with these parameters. For $N_C \geq 28$, the scaled radius of gyration at low temperature is around 0.47 Å and all carbon atoms are triply coordinated. This corresponds to cages and is consistent with the known geometry of fullerenes. For instance, buckminsterfullerene has a radius of 3.60 Å with the REBO potential, corresponding to a value of the scaled radius of gyration of 0.465 Å, a zero-temperature value that is fully consistent with the data in Fig. 1(b).

From the PTMC simulations, structures were characterized based on their values of the different order parameters R_g , A_3 , S , N_2 , and N_3 , which form a minimal set of descriptors for the clusters. At a given temperature, a specific structure can be retrieved from the sample as the one closest to the configuration with average values of these descriptors. Here, a simple Euclidean metric was used to define distances in descriptor space (see the supplementary material). Several of these most representative structures are depicted in Fig. 2 for different relevant temperatures.

At low temperature, the most representative structures of C_{28} and C_{60} , as shown in Figs. 2(a) and 2(e), are clearly those of cages with little or no topological defect. As temperature increases and reaches the 3000–4000 K range, clusters with up to 60 carbon atoms lose their aromaticity with sharp decreases in the number of triply coordinated atoms and increases in the radii of gyration. The statistical distributions of these parameters (see Fig. S2 in the supplementary material) remain very narrow around the average at low temperature but above the transition temperature become much broader, particularly for the scaled radius of gyration, showing an increased structural diversity. The configurational population in this higher temperature range corresponds to branched and dissociated structures; see Figs. 2(d) and 2(h). According to our rather loose criterion for disconnected structures (carbon–carbon distances above 3 Å), dissociated structures only become significant at temperatures above the melting range. However, at 4000 K, their proportions remain rather small, although they steadily increase above this temperature, reaching 20% and 47% at 5500 K for C_{28} and C_{60} , respectively (see Fig. S3 in the supplementary material). The continuous progression between branched and dissociated structures above the melting temperature indicates that, from a purely

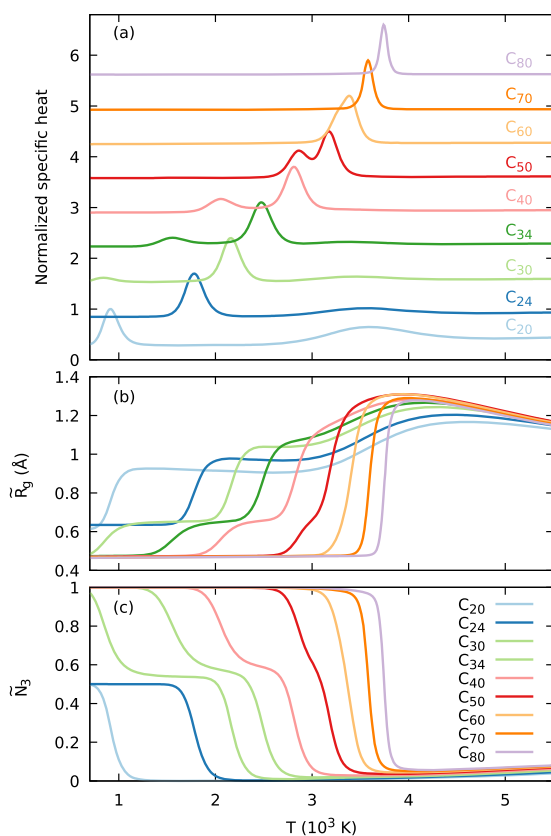


FIG. 1. Temperature dependence of various properties of pure carbon clusters: (a) specific heat normalized at its maximum, (b) average scaled gyration radius, and (c) average fraction of triply coordinated carbon atoms. The specific heat curves have been shifted vertically to improve readability.

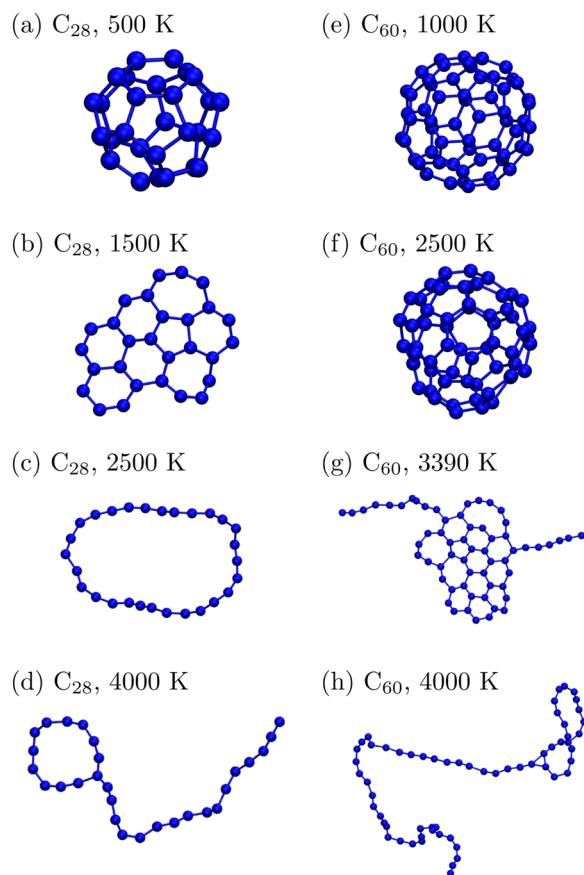


FIG. 2. Most representative structures for various pure carbon clusters at different temperatures, as defined from distances based on the minimal set of descriptors.

thermodynamical point of view, they can be considered to form a single broad family.

Smaller pure carbon clusters exhibit a different phenomenology, whose details can be inferred from the variations in the descriptors. While cages are still favored at low temperature, the substantial increase of \tilde{R}_g toward 0.64 Å and the decrease of \tilde{N}_3 toward 0.6 indicate the predominance of flakes, which is confirmed by looking at the most representative structures such as the one obtained for C_{28} at 1500 K in Fig. 2(b). Returning to C_{60} , a closer inspection of the structural features indicates that flakes are also found as the main phase but in a rather narrow temperature range, just below the melting point [see Fig. 2(g) for the most representative structure at 3390 K]. This very narrow range of stability, together with different sampling methods, explain why this phase was not seen in the earlier work by Kim and Tománek,³⁹ especially for fullerenes larger than C_{60} . However, a fourth population of structures is also visible on the variations of the scaled radius of gyration, which exhibits values between $\tilde{R}_g \approx 0.9$ and $\tilde{R}_g \approx 1.1$ Å for clusters containing 40 atoms or less. This population cannot be seen with the triply coordinated atoms as they are buried within the family of branched structures. However, a direct analysis shows that this

population corresponds to rings, as illustrated in Fig. 2(c) for C_{28} at 2500 K.

B. Effect of hydrogenation

The above results indicate that the thermodynamics of carbon clusters depends qualitatively on their size, with up to four possible phases at finite temperature. We now show that the addition of hydrogen atoms also strongly affects this thermal behavior. Figure 3(a) depicts the temperature dependence of the normalized specific heat for $C_{28}H_n$ clusters with $0 \leq n \leq 12$. As the hydrogen content increases, the main peak in the specific heat progressively increases from 1960 K in the pure cluster to 3450 K in $C_{28}H_{12}$. Conversely, the lower temperature peak marking the structural transition from cages to flakes further shifts to even lower values as more hydrogen is introduced into the system, becoming no longer discernible above $n = 3$. The broad high-temperature peak found for C_{28} near 3400 K is also very sensitive to the presence of hydrogen, as it is no longer visible already for $n = 1$.

Strong effects of hydrogen on the phases and phase changes are also found for C_{60} , the specific heats being illustrated in Fig. 3(d) for hydrogen atoms increasing in numbers from 0 to 16. The single asymmetric peak in the specific heat found for C_{60} smoothly evolves with increasing hydrogen loadings, the low-temperature shoulder becoming a distinct peak that shifts from 3390 K toward lower and lower temperature, reaching 1590 K in $C_{60}H_{10}$, while the main melting peak slightly shifts from 3390 K in the pure carbon cluster to 3780 K in $C_{60}H_{16}$.

The structural features associated with the clusters underlying the thermodynamical phases are again inferred by considering the scaled radius of gyration and the fraction of triply coordinated carbon atoms, whose variations with temperature are shown in Figs. 3(b), 3(c), 3(e), and 3(f), respectively.

Upon inspection of these quantities, both the cage and ring structures for $C_{28}H_n$ are found to be strongly destabilized by the addition of hydrogen, and for $n \geq 4$, only the flake and branched/dissociated structures remain, as illustrated on their most representative structures in Fig. 4. In $C_{60}H_n$, increasing the hydrogen loading also leads to the stabilization of the flakes to the expense of cage structures, which are even no longer found for $n \geq 12$, leaving again flakes and branched or dissociated structures as the only relevant phases. While the addition of hydrogen generally simplifies the phenomenology of melting in hydrocarbon clusters at low temperatures, it also affects the high-temperature behavior by producing greater amounts of fragments (see Fig. S3 in the supplementary material), also with a greater chemical diversity that notably includes acetylene.

C. Phase diagrams

The results obtained from our simulations can be further processed and interpreted in terms of finite temperature phase diagrams. More precisely, and as supported by the sets of representative structures depicted in Figs. 2 and 4, we distinguish cages, flakes, branched/dissociated structures, and rings. The gyration radius and fraction of triply coordinated carbon atoms suffice to assign structures from the three first families unambiguously (see Fig. S4 in the supplementary material), but for

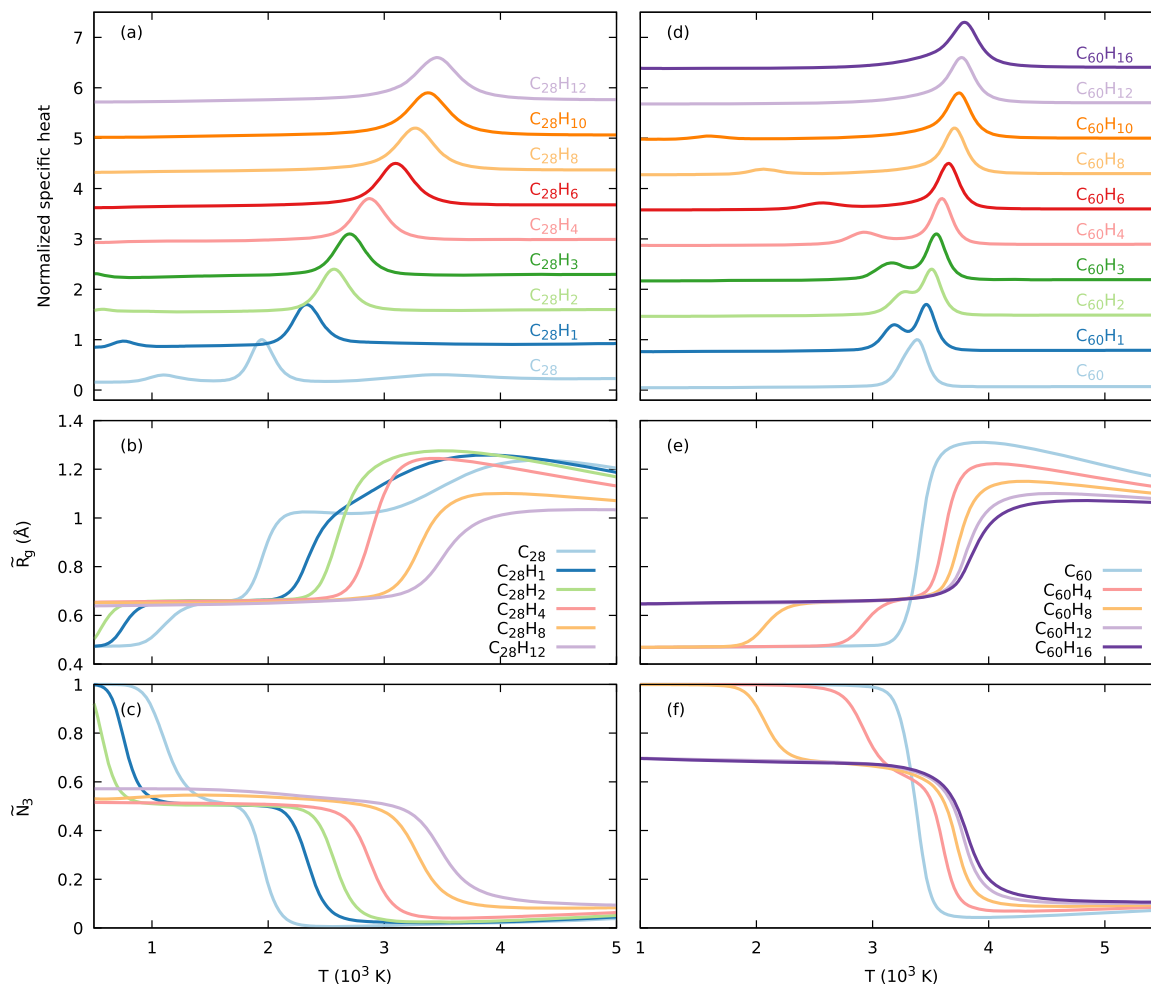


FIG. 3. Temperature dependence of various properties of hydrocarbon clusters, containing 28 (left panels) or 60 (right panels) carbon atoms: (a) and (d) normalized specific heat at its maximum, (b) and (e) scaled gyration radius, and (c) and (f) fraction of triply coordinated carbon atoms. The specific heats curves have been shifted vertically to improve readability.

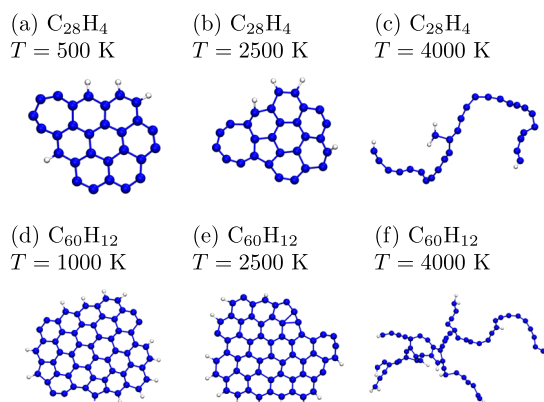


FIG. 4. Most representative structures for selected hydrocarbon clusters at different temperatures, as defined from distances based on the minimal set of descriptors.

the rings, it is the fraction $\tilde{N}_2 = N_2/N_C$ of doubly coordinated atoms that is needed in the absence of atoms with any greater coordination,

$$\text{cages: } \tilde{R}_g < 0.56,$$

$$\text{flakes: } \tilde{R}_g \geq 0.56, \tilde{N}_3 \geq 0.32,$$

$$\text{branched/dissociated: } \tilde{R}_g \geq 0.56, \tilde{N}_3 < 0.32,$$

$$\text{rings: } \tilde{N}_2 = 1.$$

The phase diagrams resulting from these definitions are represented in Fig. 5 as a double function of temperature and numbers of carbon or hydrogen atoms. Apart from minor size effects, the boundaries between the various phases are relatively smooth throughout the entire phase diagrams, suggesting that the trends inferred from the present simulations are robust.

The structural competition between the four families is usually the highest in the small size limit, rings being, for example, stabilized

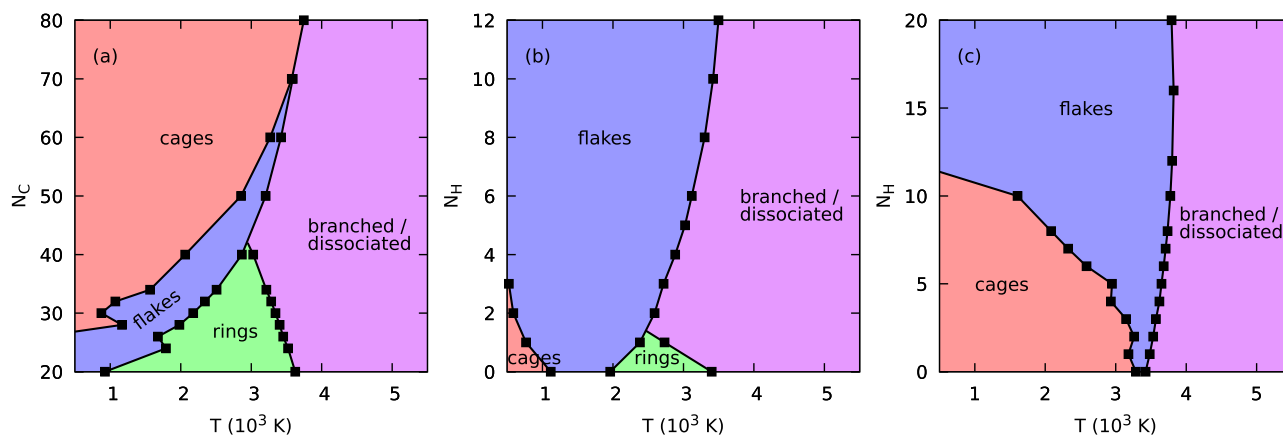


FIG. 5. Temperature and size stability diagram of (a) pure carbon clusters, (b) $C_{28}H_n$, and (c) $C_{60}H_n$ hydrocarbon clusters with $n \equiv N_H$.

by entropy ($T > 1000$ K) but only for hydrocarbon clusters having no more than 40 atoms. However, the most striking feature of these diagrams is the competition between cages and flakes, the latter being favored by hydrogen loading but disfavored by increasing number of carbon atoms. In particular, our results show that, for the present model, flakes and graphene nanoribbons are found to be nothing but metastable configurations for clusters containing more than 70 carbon atoms and that they should transform into either cages or branched structures depending on temperature.

Deeper insight into the specific phase changes can also be obtained by considering the (Landau) free energy and its variations with appropriate order parameters. As an example, we provide in the [supplementary material](#) (Fig. S5) the 1D Landau free energies of $C_{60}H_n$ with $n = 0-10$ associated with the scaled radius of gyration and the proportion \tilde{N}_3 of triply coordinated carbon atoms, at various temperatures near the phase change between cages and flakes. Close to its melting temperature of 3390 K, C_{60} exhibits two free energy minima of comparable depth, confirming that the corresponding transition is first-order-like, rounded by size effects. Another more extended minimum can also be found for the branched and dissociated structures at large gyration radii or low N_3 numbers. The energy barrier separating cages and flakes from each other is about 1.7 eV, somewhat lower than Stones–Wales rearrangement energies,⁵⁵ and remains rather stable upon moderate hydrogenation for up to $n = 8$ hydrogen atoms.

IV. CONCLUSIONS

To summarize, the present computational study provided a fairly complete statistical survey of the structures of hydrocarbon clusters at various sizes, compositions, and temperatures in the broad range of 500–5500 K covering the solid–liquid–vapor phases. In large pure carbon clusters, the results from Kim and Tománek³⁹ were recovered, with melting proceeding through the main phase change from cages to branched and dissociated structures. However, far more details could be unraveled here by scrutinizing descriptors aimed at probing separately the shape and the extent of sp^2 hybridization. In particular, the importance of graphene flakes,

which was overlooked in earlier studies, was confirmed and found to have a thermodynamical signature also in C_{60} as a melting precursor.

In smaller clusters, but also in hydrogenated compounds, the flake structures become increasingly stable to the expense of cages and the benefit of (possibly unsaturated) polycyclic aromatic hydrocarbons, already with few hydrogen atoms. Ring structures also appear to be stabilized by entropy, contributing to rather rich phase diagrams exhibiting up to three possible phase changes driven by temperature, at fixed size and composition. The structural complexity is consistent with earlier ion mobility experiments,^{24,56} and our results provide the typical ranges of excitation energies needed to access the various specific structures.

Beyond laboratory experiments, our results also have important implications in astrochemistry, where organic compounds can be heated quite significantly by absorption of single photons in the UV/visible range. This in itself would suffice to enable isomerization into a large diversity of structures, especially graphene flakes, thus contributing to different absorption and emission bands, and more generally to spectroscopic features that are much broader than the highly resolved and so specific fullerenes signatures.

Another important result of the present work is the relatively easy stabilization of polycyclic aromatic hydrocarbons upon hydrogenation of pure carbon clusters, even by moderate amounts of hydrogen. The connection between fullerene structures and planar flakes, which has been the subject of earlier works,^{46,47} is found here to be further favored by the astrophysical environment.

The present simulations at finite temperature extend the very recent survey of stable hydrocarbon structures at zero temperature (Ref. 38) and emphasize the key role of entropy in medium size clusters. However, kinetic considerations were ignored and we expect the observation time scale to play an important role on the possible characterization of the various species identified in the phase diagrams. The branched/dissociated family is particularly prone to kinetic effects, as cluster fragmentation could be irreversible depending on the experimental conditions of density and temperature. Larger scale rearrangements between cages and flakes, in the context of fullerene formation,^{46,47} would also be worth scrutinizing further, possibly through transition path sampling approaches^{57,58} but also using tools from graph theory.⁵⁹

In the astrochemical context, the internal energy of individual clusters could be transferred to other degrees of freedom through various photophysical processes, such as internal conversion but also radiation in the infrared or even optical range through the so-called Poincaré fluorescence mechanism.^{60–62} In future contributions, it will be important to account for the various competing kinetic processes and extend the present findings to the out-of-equilibrium situation of isomerizing clusters prone to radiative cooling.

SUPPLEMENTARY MATERIAL

See the [supplementary material](#) for a detailed description of the computational methods and structural parameters, temperature evolution of the distribution of structural parameters and dissociation probability, and Landau free energies along selected order parameters.

ACKNOWLEDGMENTS

Financial support by the ANR “PACHYNO” under Grant No. ANR-16-CE29-0025 is acknowledged. The authors also acknowledge the computational resources provided by the GRICAD infrastructure (<https://gricad.univ-grenoble-alpes.fr>), which is supported by Grenoble research communities.

AUTHOR DECLARATIONS

Conflict of Interest

The authors have no conflicts to disclose.

Author Contributions

Ariel Francis Perez-Mellor: Data curation (equal); Formal analysis (equal); Writing – review & editing (equal). **Pascal Parneix:** Conceptualization (equal); Funding acquisition (equal); Writing – review & editing (equal). **Florent Calvo:** Conceptualization (equal); Funding acquisition (equal); Writing – original draft (equal); Writing – review & editing (equal). **Cyril Falvo:** Conceptualization (equal); Data curation (equal); Formal analysis (equal); Funding acquisition (equal); Writing – original draft (equal); Writing – review & editing (equal).

DATA AVAILABILITY

The data that support the findings of this study are available from the corresponding author upon reasonable request.

REFERENCES

- 1 T. J. Bandoz, “Nanoporous carbon materials: From char to sophisticated 3-D graphene-like structures,” in *Nanoporous Materials for Molecule Separation and Conversion, Micro and Nano Technologies*, edited by J. Liu and F. Ding (Elsevier, 2020), Chap. 2, pp. 45–64.
- 2 G. von Helden, M.-T. Hsu, P. R. Kemper, and M. T. Bowers, “Structures of carbon cluster ions from 3 to 60 atoms: Linears to rings to fullerenes,” *J. Chem. Phys.* **95**, 3835–3837 (1991).

- 3 H. Handschuh, G. Ganteför, B. Kessler, P. S. Bechthold, and W. Eberhardt, “Stable configurations of carbon clusters: Chains, rings, and fullerenes,” *Phys. Rev. Lett.* **74**, 1095–1098 (1995).
- 4 A. Van Orden and R. J. Saykally, “Small carbon clusters: Spectroscopy, structure, and energetics,” *Chem. Rev.* **98**, 2313–2358 (1998).
- 5 K. Koyasu, T. Ohtaki, N. Hori, and F. Misaizu, “Isomer-resolved dissociation of small carbon cluster cations, C_7^+ – C_{10}^+ ,” *Chem. Phys. Lett.* **523**, 54–59 (2012).
- 6 R. Moriyama, J. W. J. Wu, M. Nakano, K. Ohshimo, and F. Misaizu, “Small carbon nano-onions: An ion mobility mass spectrometric study,” *J. Phys. Chem. C* **122**, 5195–5200 (2018).
- 7 C. J. Hull, S. L. Raj, and R. J. Saykally, “The liquid state of carbon,” *Chem. Phys. Lett.* **749**, 137341 (2020).
- 8 A. Léger and J. L. Puget, “Identification of the ‘unidentified’ IR emission features of interstellar dust,” *Astron. Astrophys.* **137**, L5–L8 (1984).
- 9 L. J. Allamandola, A. G. G. M. Tielens, and J. R. Barker, “Polycyclic aromatic hydrocarbons and the unidentified infrared emission bands—Auto exhaust along the milky way,” *Astrophys. J.* **290**, L25–L28 (1985).
- 10 A. G. G. M. Tielens, “Interstellar polycyclic aromatic hydrocarbon molecules,” *Annu. Rev. Astron. Astrophys.* **46**, 289–337 (2008).
- 11 P. F. Bernath, K. H. Hinkle, and J. J. Keady, “Detection of C_5 in the circumstellar shell of IRC+10216,” *Science* **244**, 562–564 (1989).
- 12 J. P. Maier, N. M. Lakin, G. A. H. Walker, and D. A. Bohlender, “Detection of C_3 in diffuse interstellar clouds,” *Astrophys. J.* **553**, 267–273 (2001).
- 13 J. Cami, J. Bernard-Salas, E. Peeters, and S. E. Malek, “Detection of C_{60} and C_{70} in a young planetary nebula,” *Science* **329**, 1180–1182 (2010).
- 14 K. Sellgren, M. W. Werner, J. G. Ingalls, J. D. T. Smith, T. M. Carleton, and C. Joblin, “ C_{60} in reflection nebulae,” *Astrophys. J. Lett.* **722**, L54 (2010).
- 15 L. M. Hobbs, D. G. York, T. P. Snow, T. Oka, J. A. Thorburn, M. Bishop, S. D. Friedman, B. J. McCall, B. Rachford, P. Sonnentrucker, and D. E. Welty, “A catalog of diffuse interstellar bands in the spectrum of HD 204827,” *Astrophys. J.* **680**, 1256–1270 (2008).
- 16 M. Steglich, J. Bouwman, F. Huisken, and T. Henning, “Can neutral and ionized polycyclic aromatic hydrocarbons be carriers of the ultraviolet extinction bump and the diffuse interstellar bands?,” *Astrophys. J.* **742**, 2 (2011).
- 17 L. Gavilan, K. C. Le, T. Pino, I. Alata, A. Giuliani, and E. Dartois, “Polyaromatic disordered carbon grains as carriers of the UV bump: Far-UV to mid-IR spectroscopy of laboratory analogs,” *Astron. Astrophys.* **607**, A73 (2017).
- 18 M. A. Bonnin, C. Falvo, F. Calvo, T. Pino, and P. Parneix, “Simulating the structural diversity of carbon clusters across the planar-to-fullerene transition,” *Phys. Rev. A* **99**, 042504 (2019).
- 19 C. Dubosq, C. Falvo, F. Calvo, M. Rapacioli, P. Parneix, T. Pino, and A. Simon, “Mapping the structural diversity of C_{60} carbon clusters and their infrared spectra,” *Astron. Astrophys.* **625**, L11 (2019).
- 20 C. Dubosq, F. Calvo, M. Rapacioli, E. Dartois, T. Pino, C. Falvo, and A. Simon, “Quantum modeling of the optical spectra of carbon cluster structural families and relation to the interstellar extinction UV bump,” *Astron. Astrophys.* **634**, A62 (2020).
- 21 A. Omont and H. F. Bettinger, “Intermediate-size fullerenes as degradation products of interstellar polycyclic aromatic hydrocarbons,” *Astron. Astrophys.* **650**, A193 (2021).
- 22 M. C. McCarthy and B. A. McGuire, “Aromatics and cyclic molecules in molecular clouds: A new dimension of interstellar organic chemistry,” *J. Phys. Chem. A* **125**, 3231–3243 (2021).
- 23 J. Rademacher, E. S. Reedy, and E. K. Campbell, “Electronic spectroscopy of monocyclic carbon ring cations for astrochemical consideration,” *J. Phys. Chem. A* **126**, 2127–2133 (2022).
- 24 N. G. Gotts, G. von Helden, and M. T. Bowers, “Carbon cluster anions: Structure and growth from C_5^- to C_{62}^- ,” *Int. J. Mass Spectrom. Ion Processes* **149–150**, 217–229 (1995).
- 25 P. R. Taylor, E. Bylaska, J. H. Weare, and R. Kawai, “ C_{20} : Fullerene, bowl or ring? New results from coupled-cluster calculations,” *Chem. Phys. Lett.* **235**, 558–563 (1995).
- 26 C. Zhang, X. Xu, H. Wu, and Q. Zhang, “Geometry optimization of C_n ($n = 2–30$) with genetic algorithm,” *Chem. Phys. Lett.* **364**, 213–219 (2002).

- ²⁷W. Cai, N. Shao, X. Shao, and Z. Pan, "Structural analysis of carbon clusters by using a global optimization algorithm with Brenner potential," *J. Mol. Struct.: THEOCHEM* **678**, 113–122 (2004).
- ²⁸N. Shao, Y. Gao, S. Yoo, W. An, and X. C. Zeng, "Search for lowest-energy fullerenes: C₉₈ to C₁₁₀," *J. Phys. Chem. A* **110**, 9523 (2006).
- ²⁹N. Shao, Y. Gao, and X. C. Zeng, "Search for lowest-energy fullerenes 2: C₃₈ to C₈₀ and C₁₁₂ to C₁₂₀," *J. Phys. Chem. C* **111**, 17671–17677 (2007).
- ³⁰D. P. Kosimov, A. A. Dzhurakhalov, and F. M. Peeters, "Theoretical study of the stable states of small carbon clusters C_n (n = 2–10)," *Phys. Rev. B* **78**, 235433 (2008).
- ³¹D. P. Kosimov, A. A. Dzhurakhalov, and F. M. Peeters, "Carbon clusters: From ring structures to nanographene," *Phys. Rev. B* **81**, 195414 (2010).
- ³²T. W. Yen and S. K. Lai, "Use of density functional theory method to calculate structures of neutral carbon clusters C_n (3 ≤ n ≤ 24) and study their variability of structural forms," *J. Chem. Phys.* **142**, 084313 (2015).
- ³³S. K. Lai, I. Setiyawati, T. W. Yen, and Y. H. Tang, "Studying lowest energy structures of carbon clusters by bond-order empirical potentials," *Theor. Chem. Acc.* **136**, 20 (2016).
- ³⁴A. J. C. Varandas, "Even numbered carbon clusters: Cost-effective wavefunction-based method for calculation and automated location of most structural isomers," *Eur. Phys. J. D* **72**, 134 (2018).
- ³⁵B. W. Clare and D. L. Kepert, "Structures, stabilities and isomerism in C₆₀H_n, n = 2–36. A comparison of the AM1 Hamiltonian and density functional techniques," *J. Mol. Struct.: THEOCHEM* **622**, 185–202 (2003).
- ³⁶A. Bihlmeier, D. P. Tew, and W. Klopper, "Low energy hydrogenation products of extended π systems C_nH_{2x}: A density functional theory search strategy, benchmarked against CCSD(T), and applied to C₆₀," *J. Chem. Phys.* **129**, 114303 (2008).
- ³⁷H. Tachikawa and T. Iyama, "Electronic structures and large spectrum shifts in hydrogenated fullerenes: Density functional theory study," *Thin Solid Films* **554**, 148–153 (2014).
- ³⁸S. V. Lepeshkin, V. S. Baturin, A. S. Naumova, and A. R. Oganov, "'Magic' molecules and a new look at chemical diversity of hydrocarbons," *J. Phys. Chem. Lett.* **13**, 7600–7606 (2022).
- ³⁹S. G. Kim and D. Tománek, "Melting the fullerenes: A molecular dynamics study," *Phys. Rev. Lett.* **72**, 2418–2421 (1994).
- ⁴⁰J. M. L. Martin, J. El-Yazal, and J.-P. François, "On the structure and vibrational frequencies of C₂₀," *Chem. Phys. Lett.* **248**, 345–352 (1996).
- ⁴¹A. Allouch, J. Mougenot, S. Prasanna, A. Michau, M. Seydou, F. Maurel, P. Brault, and K. Hassouni, "Statistical abundance and stability of carbon nanostructures by combined condensation-annealing molecular dynamics simulations," *Comput. Theor. Chem.* **1201**, 113252 (2021).
- ⁴²D. Furman, F. Naumkin, and D. J. Wales, "Energy landscapes of carbon clusters from tight-binding quantum potentials," *J. Phys. Chem. A* **126**, 2342–2352 (2022).
- ⁴³S. Dutta and S. K. Pati, "Novel properties of graphene nanoribbons: A review," *J. Mater. Chem.* **20**, 8207–8223 (2010).
- ⁴⁴V. Georgakilas, J. A. Perman, J. Tucek, and R. Zboril, "Broad family of carbon nanoallotropes: Classification, chemistry, and applications of fullerenes, carbon dots, nanotubes, graphene, nanodiamonds, and combined superstructures," *Chem. Rev.* **115**, 4744–4822 (2015).
- ⁴⁵H. Wang, H. S. Wang, C. Ma, L. Chen, C. Jiang, C. Chen, X. Xie, A.-P. Li, and X. Wang, "Graphene nanoribbons for quantum electronics," *Nat. Rev. Phys.* **3**, 791–802 (2021).
- ⁴⁶O. Berné and A. G. G. M. Tielens, "Formation of buckminsterfullerene (C₆₀) in interstellar space," *Proc. Natl. Acad. Sci. U. S. A.* **109**, 401–406 (2012).
- ⁴⁷O. Berné, J. Montillaud, and C. Joblin, "Top-down formation of fullerenes in the interstellar medium," *Astron. Astrophys.* **577**, A133 (2015).
- ⁴⁸R. H. Swendsen and J.-S. Wang, "Replica Monte Carlo simulation of spin-glasses," *Phys. Rev. Lett.* **57**, 2607–2609 (1986).
- ⁴⁹D. W. Brenner, O. A. Shenderova, J. A. Harrison, S. J. Stuart, B. Ni, and S. B. Sinnott, "A second-generation reactive empirical bond order (REBO) potential energy expression for hydrocarbons," *J. Phys.: Condens. Matter* **14**, 783 (2002).
- ⁵⁰S. Kumar, J. M. Rosenberg, D. Bouzida, R. H. Swendsen, and P. A. Kollman, "The weighted histogram analysis method for free-energy calculations on biomolecules. I. The method," *J. Comput. Chem.* **13**, 1011–1021 (1992).
- ⁵¹R. Poteau, F. Spiegelmann, and P. Labastie, "Isomerisation and phase transitions in small sodium clusters," *Z. Phys. D: At. Mol. Clust.* **30**, 57–68 (1994).
- ⁵²V. Blavatska and W. Janke, "Shape anisotropy of polymers in disordered environment," *J. Chem. Phys.* **133**, 184903 (2010).
- ⁵³F. Calvo, F. Chiro, F. Albrieux, J. Lemoine, Y. O. Tsybin, P. Pernot, and P. Dugourd, "Statistical analysis of ion mobility spectrometry. II. Adaptively biased methods and shape correlations," *J. Am. Soc. Mass Spectrom.* **23**, 1279–1288 (2012).
- ⁵⁴M. Fixman, "Radius of gyration of polymer chains," *J. Chem. Phys.* **36**, 306–310 (1962).
- ⁵⁵L. G. Zhou and S.-Q. Shi, "Formation energy of Stone–Wales defects in carbon nanotubes," *Appl. Phys. Lett.* **83**, 1222–1224 (2003).
- ⁵⁶S. Lee, N. Gotts, G. von Helden, and M. T. Bowers, "Structures of C_nH_x⁺ molecules for n ≤ 22 and x ≤ 5: Emergence of PAHs and effects of dangling bonds on conformation," *J. Phys. Chem. A* **101**, 2096–2102 (1997).
- ⁵⁷C. Dellago, P. G. Bolhuis, F. S. Csajka, and D. Chandler, "Transition path sampling and the calculation of rate constants," *J. Chem. Phys.* **108**, 1964–1977 (1998).
- ⁵⁸R. Cabriolu, K. M. Skjeltved Refsnes, P. G. Bolhuis, and T. S. van Erp, "Foundations and latest advances in replica exchange transition interface sampling," *J. Chem. Phys.* **147**, 152722 (2017).
- ⁵⁹A. F. Perez-Mellor and R. Spezia, "Determination of kinetic properties in unimolecular dissociation of complex systems from graph theory based analysis of an ensemble of reactive trajectories," *J. Chem. Phys.* **155**, 124103 (2021).
- ⁶⁰A. Léger, P. Boissel, and L. d'Hendecourt, "Predicted fluorescence mechanism in highly isolated molecules: The Poincaré fluorescence," *Phys. Rev. Lett.* **60**, 921–924 (1988).
- ⁶¹S. Martin, J. Bernard, R. Brédy, B. Concina, C. Joblin, M. Ji, C. Ortega, and L. Chen, "Fast radiative cooling of anthracene observed in a compact electrostatic storage ring," *Phys. Rev. Lett.* **110**, 063003 (2013).
- ⁶²O. Lacinbala, F. Calvo, C. Dubosq, C. Falvo, P. Parneix, M. Rapacioli, A. Simon, and T. Pino, "Radiative relaxation in isolated large carbon clusters: Vibrational emission versus recurrent fluorescence," *J. Chem. Phys.* **156**, 144305 (2022).